Evolution of Fractal Structures in Dislocation Ensembles during Plastic Deformation

A. Vinogradov,[1,*] I. S. Yasnikov,[1] and Y. Estrin[2]

[1]*Laboratory for the Physics of Strength of Materials and Intelligent Diagnostic Systems, Togliatti State University, Togliatti 445667, Russia*

[2]*Centre for Advanced Hybrid Materials, Department of Materials Engineering, Monash University, Clayton VIC 3800, Australia*

(Received 8 February 2012; published 15 May 2012)

Based on the irreversible thermodynamics approach to dislocation plasticity of metals, a simple description of the dislocation density evolution and strain hardening was suggested. An analytical expression for the fractal dimension (FD) of a cellular (or tangled) dislocation structure evolving in the course of plastic deformation was obtained on the basis of the dislocation model proposed. This makes it possible to trace the variation of FD of the dislocation cell structure with strain by just measuring the macroscopic stress-strain curve. The FD behavior predicted in this way showed good agreement with the experimentally measured FD evolution at different stages of deformation of a Ni single crystal and a Cu polycrystal. One new result following from the present model is that the FD of the bulk dislocation structure in a deforming metal peaks at a certain strain close to the onset of necking. The significance of fractal analysis as an informative index to follow the spatial evolution of dislocation structures approaching the critical state is highlighted.

DOI: 10.1103/PhysRevLett.108.205504 PACS numbers: 62.20.F−, 05.45.Df, 05.70.Ln, 81.40.Ef

Being a highly dissipative process, plastic deformation occurs in a broad variety of patterns, which may be different with regard to their inner length scale or, by contrast, exhibit a scale-free behavior [1]. Characterizing and predicting patterning in the dislocation population that accompanies plastic deformation of crystalline solids is a particularly challenging problem. Fractal analysis is a potent tool to account for multiscale features and relate the macroscopic properties of a material to its dislocation structure.

Plastic deformation in a metallic sample produces a characteristic relief on its surface. It is clear intuitively that the features of the surface relief are affected by the microstructure evolving within the bulk, so that fractal dimension (FD) of the surface topography must be related to that of the bulk dislocation structure. Accordingly, both bulk and surface measurements have been used to determine the evolution of FD in literature. Zaiser *et al.* [2] have measured the Hausdorf FD from the surface profile quantified by atomic force microscopy (AFM) and scanning white-light interferometry (SWLI) in copper polycrystals deformed up to 25%. With both techniques used, the FD was found to increase from 2.0 to 2.3 and then to saturate at this level. These results correlate well with the findings by transmission electron microscopy (TEM) [3] that self-affine cellular dislocation patterns occur at various length scales in the bulk of a deforming crystal. The observed FDs (box and gap) were found to show an increase, while no apparent plateau region could be found at large strain. The evolution of self-affine surface roughness during early stages of deformation was also studied on KCl single crystals [4]. It was found that during the easy glide (stage I) deformation the FD shows a slight tendency to grow, followed by a rapid rise in stage II of strain hardening. Finally, by using AFM profiling of deformed surface of a nickel single crystal Meissner *et al.* [5] observed a similar behavior of FD in stages I and II.

Overall, the available experimental data indicate that (i) both the deformation-induced surface patterns and the underlying dislocation structures in the bulk are self-affine, (ii) the FD of the dislocation pattern changes slightly during stage I of strain hardening in single crystals and tends to increase sharply at the onset of pronounced strain hardening in stage II and (iii) the FD tends to saturate with strain, although genuine saturation could not be established conclusively. To add to this uncertainty, the results by Kuznetsov *et al.* [6] suggest that the FD value peaks just before fracture. Most of the currently available results cover early deformation stages and do not extend to the point of necking, which is one of the critical points of interest on the stress-strain curve.

The present study aims at shedding more light on the evolution of the FD, particularly by extending the strain range investigated to the necking point. An important ingredient of the intended FD analysis is a reliable description of the dislocation density evolution. We shall develop such a description using an irreversible thermodynamics approach. The rationale behind the earlier research, seeking insight in the evolution of the dislocation structure through FD measurements, also applies to the present study. While it is not our goal here to resolve the question of whether the quantities measured at the surface can represent the behavior of the bulk, some of the results reported below do support this hypothesis.

We consider plastic deformation from the standpoint of evolution of an open system approaching a steady state. The total entropy flux is described by $dS = d_iS + d_eS$ where d_iS is the entropy production due to changes in the internal microstructure (always a positive quantity) and d_eS is the entropy flux due to heat exchange with the thermal bath. Following a general formalism proposed by Prigogine [7], Huang *et al.* [8] developed an irreversible thermodynamics approach to dislocation-based modeling of strain hardening. They related the entropy production d_iS associated with a shear strain increment $d\gamma$ to the energy dissipated due to dislocation generation (dW^+), motion ($dW^=$) and annihilation (dW^-) in the bulk of the deforming metal as $d_iS = \frac{1}{T}(dW^+ + dW^= + dW^-)$, where T is the absolute temperature. The energy dissipation due to generation and annihilation of dislocations is associated with the dislocation line energy [8] as $dW^+ = \frac{1}{2}Gb^2d\rho^+$ and $dW^- = \frac{1}{2}Gb^2d\rho^-$, where $d\rho^+$ and $d\rho^-$ are the increments of dislocation densities for dislocation production and recovery (annihilation), respectively, G is the shear modulus, and b is the magnitude of the Burgers vector of a dislocation. The term $dW^=$ is expressed as $dW^= = \tau b\langle l\rangle d\rho^+$ where $\langle l\rangle$ is the dislocation mean free path related to the average dislocation spacing as $\langle l\rangle \sim 1/\sqrt{\rho}$ with $\rho = \rho^+ - \rho^-$ being the total dislocation density, and τ denoting the shear stress acting in the dislocation glide plane [9]. According to the Taylor relation, the shear stress τ scales with $\sqrt{\rho}$ as

$$\tau = \alpha Gb\sqrt{\rho} \tag{1}$$

where α is a numerical factor (typically ~0.5) [10]. The friction stress, which stems from interactions of a gliding dislocation with the Peierls relief and point defects, can be assumed to be negligible, at least for pure fcc metals, and it has been dropped. Equation (1) is rather universal. Indeed, not only do virtually all conceivable dislocation-dislocation interaction mechanisms lead to this relation, but it is also supported by a wealth of experimental data and computer simulations using discrete dislocation dynamics [11]. Hence, $dW^=$ reads as $dW^= = \alpha Gb^2d\rho^+$. Combining the expressions for dW^+, dW^- and $dW^=$ one obtains

$$d_iS = \frac{(1+2\alpha)Gb^2}{2T}d\rho + \frac{(2+2\alpha)Gb^2}{2T}d\rho^-. \tag{2}$$

The entropy flux d_eS is associated with dissipation as heat of most of the mechanical work $\tau d\gamma$ upon a strain increment $d\gamma$ [7]:

$$d_eS = -\frac{\tau d\gamma}{T}. \tag{3}$$

During deformation of a crystal, dislocations are generated, travel a distance $\langle l\rangle$, and get annihilated. These processes result in a stress-strain behavior characterized by strain hardening. Dislocation patterns start developing early on, after the onset of plastic flow. Already in stage II deformation multiple slip systems are activated giving rise to tangled dislocation networks evolving to stable cell configurations. These patterns consist of dislocation-rich ''cell walls'' separating cell interiors, which are less populated with dislocations. We shall not consider fine details of dislocation structure or distinguish between tangled dislocation networks and dislocation cell arrangements.

When dislocations are organized in a fashion discussed above, a ''composite model'' [12,13] can be used to describe the mechanical response. The dislocation structure is considered to be composed of the cell-wall ''phase'' with the volume fraction f_w and the interior ''phase'' with the volume fraction f_c. Applying a rule of mixtures, the shear stress τ is written as

$$\tau = f_w\tau_w + f_c\tau_c = f_w\alpha Gb\sqrt{\rho_w} + f_c\alpha Gb\sqrt{\rho_c}. \tag{4}$$

Here the subscripts w and c stand for cell walls and cell interiors, respectively, and ρ_w and ρ_c are the dislocation densities in the two phases. Obviously, $f_w + f_c = 1$ holds.

Mechanisms of formation of a cellular dislocation structure are still not fully understood [4], but what has transpired from the vast body of experimental evidence, based chiefly on TEM observations, is that the average dislocation cell size $\langle\lambda\rangle$ scales inversely with the square root of $\rho = f_w\rho_w + f_c\rho_c$; this scaling law can be written as [14] $\rho = a/\langle\lambda\rangle^2$, where a is a proportionality coefficient. The ρ_w value is considered to obey a similar scaling relation, but with a different coefficient a_w: $\rho_w = a_w/\langle\lambda\rangle^2$. Combining the last three equations, one obtains $a/\langle\lambda\rangle^2 = a_w/\langle\lambda\rangle^2 + f_c\rho_c$, from which one can easily recognize the proportionality between ρ_c and ρ_w: $\rho_c = \frac{a-a_w}{f_c}\rho_w = \beta\rho_w$. This linear relation between ρ_c and ρ_w, which holds as long as variation with strain of f_c can be disregarded, is in good agreement with the results reported by Mughrabi [12] on the basis of the composite model [13]—the very model we use. For realistic dislocation configurations $\rho_w \gg \rho_c$ holds, and one can replace ρ_w with ρ in Eq. (4), which then takes the form

$$\tau = \alpha Gb\left(\frac{f_w}{\langle\lambda\rangle} + \sqrt{\beta}f_c\sqrt{\rho_w}\right). \tag{5}$$

Accordingly, Eq. (3) can be rewritten as

$$d_eS = -\left(\sqrt{\beta}f_c\sqrt{\rho} + \frac{f_w}{\langle\lambda\rangle}\right)\frac{\alpha Gbd\gamma}{T}. \tag{6}$$

Combining Eqs. (2) and (6) and one obtains

$$\frac{dS}{d\gamma} = \frac{(1+2\alpha)Gb^2}{2T}\frac{d\rho}{d\gamma} + \frac{(2+2\alpha)Gb^2}{2T}\frac{d\rho^-}{d\gamma} - \left(\sqrt{\beta}f_c\sqrt{\rho} + \frac{f_w}{\langle\lambda\rangle}\right)\frac{\alpha Gb}{T}. \tag{7}$$

To proceed further, we assume dislocation annihilation by second-order kinetics, as two dislocations are involved in an elementary annihilation event;

$$\frac{d\rho^-}{dt} = \rho^2b^2\nu_0e^{-(\Delta G/k_BT)}. \tag{8}$$

Here ν_0 is the preexponential factor of the order of the Debye frequency, ΔG is the activation energy for dislocation climb (assumed to be the governing mechanism of annihilation), which can be identified with the activation energy for self-diffusion, and k_B is the Boltzmann constant. It was tacitly assumed above that annihilation mainly occurs in the cell walls and involves the dislocation density ρ_w, which was replaced with ρ in Eq. (8). Using the Orowan relation $\dot{\gamma} = \rho b \langle V \rangle$, with $\langle V \rangle$ denoting the average dislocation glide velocity, one obtains

$$\frac{d\rho^-}{d\gamma} = \frac{\rho b \nu_0}{\langle V \rangle} e^{-(\Delta G/k_B T)}. \tag{9}$$

Finally, by combining Eqs. (7) and (9) an explicit relation between the overall entropy change during plastic deformation and the total dislocation density ρ is obtained:

$$\frac{dS}{d\gamma} = \frac{(1+2\alpha)Gb^2}{2T}\frac{d\rho}{d\gamma} + \frac{(2+2\alpha)Gb^2}{2T}\frac{\rho b \nu_0}{\langle V \rangle} e^{-(\Delta G/k_B T)} - \left(\sqrt{\beta} f_c \sqrt{\rho} + \frac{f_w}{\langle \lambda \rangle}\right)\frac{\alpha G b}{T}. \tag{10}$$

Thermodynamic systems evolve to their steady state, albeit a nonequilibrium one, which is defined by the condition $dS = 0$, thus yielding a familiar evolution equation for ρ:

$$\frac{d\rho}{d\gamma} = \frac{k_0}{b\langle \lambda \rangle} + \frac{k_1\sqrt{\rho}}{b} - k_2 \rho, \tag{11}$$

where

$$k_0 = \frac{2\alpha f_w}{1+2\alpha}, \qquad k_1 = \frac{2\alpha\sqrt{\beta} f_c}{1+2\alpha}, \qquad k_2 = \frac{2+2\alpha}{1+2\alpha}\frac{b\nu_0}{\langle V \rangle} e^{(\Delta G/k_B T)}. \tag{12}$$

Equation (11) recovers the evolution equation obtained by Kocks, Mecking, and Estrin [10,15–17] in a phenomenological way. The coefficients k_0, k_1, and k_2 in their evolution equation have been reinterpreted here in terms of the two-phase model. The dislocation density evolution model in this simplified form was promoted in a number of publications [10,17] and was further developed by many researchers, cf. [18]. By integrating Eq. (11) the average dislocation density can be found as a function of strain at a given T and $\dot{\varepsilon}$. Then, employing Eq. (1), the stress-strain curve in the plastic regime can be obtained. Simple and effective recipes for identifying the parameters k_1 and k_2 from strain hardening data can be found in [15]. An adequate description of deformation stages beyond Stage III requires a detailed two-internal variable approach [19].

Based on TEM observations, Zaiser *et al.* [20] demonstrated that dislocation cell structures in fcc single crystals can be seen as self-similar fractals which are characterized by power-law distributions of cell sizes λ

$$N(\lambda > \Lambda) \propto \Lambda^{-D} \tag{13}$$

where D is the FD. Groma *et al.* [21] developed a stochastic two-dimensional model of microstructure evolution, derived from the properties of individual dislocations. Their numerical results appeared to be consistent with the fractal character of the dislocation cell structures developed. Koslowski *et al.* [22] drew similar conclusions from phase-field simulations of a two-dimensional model of dislocation microstructure development with strain, which support the experimental data reported in [20]. The probability $p(\lambda)$ for the size of a given dislocation cell to range between λ and $\lambda + d\lambda$ is therefore given as $p(\lambda) = D\lambda_{\min}^D \lambda^{-D-1}$. The average cell size is found as

$$\langle \lambda \rangle = \int_{\lambda_{\min}}^{\infty} \lambda p(\lambda) d\lambda = \frac{D}{D-1}\lambda_{\min} \tag{14}$$

where the lower cutoff cell size $\lambda_{\min}$ introduced to normalize the distribution is defined from a generic scaling relationship $\lambda_{\min} = \zeta G b/\tau$, where ζ is the proportionality coefficient which is supposed to be close to unity [20] and is dropped in what follows. Recalling Eq. (1) again, $\lambda_{\min}$ can be expressed as $\lambda_{\min} = 1/\alpha\sqrt{\rho}$ and Eq. (14) can be rewritten as

$$\langle \lambda \rangle = \lambda_{\min}\frac{D}{D-1} = \frac{1}{\alpha\sqrt{\rho}}\frac{D}{D-1}. \tag{15}$$

Upon substitution of this expression in the evolution equation for ρ, Eq. (11), one has

$$\frac{d\rho}{d\gamma} = \left(\alpha k_0 \frac{D-1}{D} + k_1\right)\frac{\sqrt{\rho}}{b} - k_2\rho. \tag{16}$$

Changing the variables and using the Taylor conversion factor M: $\gamma = \varepsilon \cdot M$ and $\tau = \sigma/M$, Eq. (16) is transformed to the following equation for the variation of the axial stress σ as a function of tensile strain ε:

$$\frac{2}{M^2}\frac{d\sigma}{d\varepsilon} + \frac{k_2}{M}\sigma = \alpha G\left(\alpha k_0 \frac{D-1}{D} + k_1\right). \tag{17}$$

It should be noted that this equation is at variance with the ''classical'' phenomenological one cited above in that the coefficients are no longer constants. Indeed, in the present approach the FD is a function of strain: $D = D(\varepsilon)$. The general solution of Eq. (17) is expressed as

$$\sigma(\varepsilon) = e^{-(k_2 M\varepsilon/2)}\left(\int_\varepsilon \left(\frac{1}{2}\alpha G M^2\left(\alpha k_0 + k_1 - \frac{\alpha k_0}{D(\varepsilon)}\right)e^{k_2 M\varepsilon/2}\right)d\varepsilon + C\right), \tag{18}$$

where the constant C is determined by the initial conditions [e.g., $\sigma(0) = 0$ and $D(0) = 1$]. An analytical solution for $D(\varepsilon)$ or $\sigma(\varepsilon)$ is hardly possible. However, $D(\varepsilon)$ can be directly expressed as a function of experimentally measurable quantities from Eq. (17):

$$D = \frac{\alpha k_0}{\alpha k_0 + k_1 - \frac{1}{\alpha M G}\left(\frac{2}{M}\frac{d\sigma}{d\varepsilon} + k_2\sigma\right)}. \tag{19}$$

That is to say the evolution of the FD is governed by the strain hardening law, i.e., by the form of the function $\sigma(\varepsilon)$ or $\theta = d\sigma(\varepsilon)/d\varepsilon$. (Note that the values of the coefficients k_0, k_1, and k_2 can be found from the same data.) This formula provides direct access to the FD of the dislocation structure through the macroscopic stress-strain curve and is pivotal for subsequent analysis.

To verify the model approach, the FD $D(\varepsilon)$ was determined from Eq. (19) by using our experimental data on the deformation behavior of a nickel single crystal oriented for easy glide (the tensile axis was close to the crystallographic orientation [123]). The results are shown in Fig. 1. Also presented are the data reported by Meissner *et al.* [5] from AFM surface profiles of a similar deformed Ni single crystal. We note a close correspondence between the FD behavior obtained by the two methods in the low strain region where small-scale features related to individual dislocation slip lines determine surface topography. This agreement supports the hypothesis that surface topography provides clues to the dislocation patterns formed in the bulk of a deforming metal [23] and adds to the arguments based on the discrete dislocation dynamics computations [24] and analytical modeling [25].

The model presented captures the salient features of the FD variation known from literature: (i) steady behavior during easy glide and (ii) a tendency to increase with strain beyond this deformation stage. The most intriguing prediction of the model is the appearance of a pronounced maximum in the $D(\varepsilon)$ dependence at fairly large strains prior to onset of necking, Fig. 1. Unfortunately, the experimental data on Ni are limited to relatively small strains, so that this specific model prediction—the occurrence of a peak in the FD—could not be verified on the basis of strain hardening data. We therefore performed independent measurements using pure 99.98% polycrystalline copper annealed at 1077 K for 2 h in vacuum. The specimens for tensile testing were prepared to an ASTM E08-91 standard sheet-type geometry with a gauge length of 10 mm.

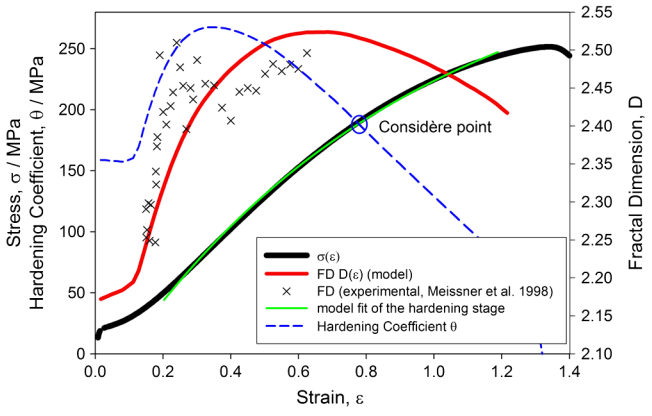

FIG. 1 (color online). Stress-strain curve for Ni single crystal (own data); the green line shows the theoretical fit of the strain hardening portion of the curve. The data points for FD obtained by Meissner *et al.* [5] are plotted for comparison.

They were then mechanically and electrolytically polished to a mirrorlike finish. Uniaxial tensile straining was at a constant nominal strain rate of 6×10^{-4} s^{-1}. Starting from a strain of 15% the tests were repeatedly interrupted for surface observations.

The surface topography was quantified for each strain level with a SWLI Nikon MicroMap microscope having lateral X-Y resolution of 500 nm and vertical Z resolution of less than 1 nm. The X-Y area of observation was set at 0.12×0.12 mm^2. Averaging of the results of FD measurements over five well-spaced images taken from different locations in the middle part of the specimen surface was done. All surface profiles were processed before analysis to remove effects of macroscopic surface curvature. Three identical specimens were tested under the same loading conditions. The surface profiles can be quantified in various ways [26,27] which have been critically reviewed in [3,28,29]. In the present work, the "box-counting dimension" was obtained by covering the 3D data set $Z(x, y)$ with a grid of boxes with edge length r and counting the number of boxes $N(r)$ which contain at least one element of the surface profile. A power-law behavior defines the box-counting dimension D_B as $D_B = \lim_{r\to 0} \frac{\log N(r)}{\log(1/r)}$. The slope in the plot of $\log[N(r)]$ vs $\log(1/r)$ gives the FD. Experimental results are plotted in Fig. 2; circles with different color refer to three different specimens. The error bars reflect the scatter of fractal exponents obtained from different surface profiles taken at the same strain. The inset displays data adapted from Ref. [3] for a similar copper polycrystal. The FD calculated using the tensile data for copper is shown by the solid red lines. It is evident that the model accounts for the experimental findings with a fair degree of accuracy.

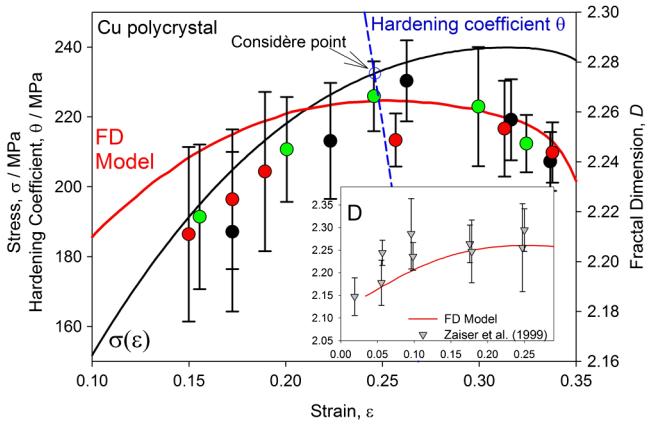

FIG. 2 (color online). Fragment of the strain hardening curve of polycrystalline copper and experimental results of FD measurements from surface profiles. The model FD calculated from the stress-strain curve is shown by the red line. The dashed line shows a fragment of the strain dependence of the strain hardening coefficient used to determine the onset of necking based on the Considère criterion. The experimental FD curve for copper obtained by Zaiser *et al.* [3] is plotted in the inset.

Importantly, the FD curve derived from our model exhibits a maximum at a certain strain close to the point of tensile instability determined by the Considère criterion $\sigma = d\sigma/d\varepsilon$ and then drops off slightly. The FD derived by AFM measurements shows a similar behavior. The latter decrease of FD is indicative of a reduction in the degree of chaos in the system with increasing role of recovery and slip coarsening in stage III deformation prior to final macroscopic strain localization in a neck.

The observation that occurrence of a peak in FD may be a precursor of failure is of great practical importance, as it makes the FD analysis an important diagnostic tool. This is confirmed in *in situ* acoustic emission measurements reflecting structural rearrangements and transition to failure in Ni and Cu crystals. These supporting results will be discussed in a forthcoming publication.

In conclusion, the irreversible thermodynamics approach to dislocation-based plasticity of metals proposed by Huang *et al.* [8], which we adopted with some modifications, leads to a simple description of the dislocation density evolution and strain hardening. It recovers the well-known KME equation, but redefines the coefficients in that equation. An analytical expression for the evolution of FD of the cellular (or tangled) dislocation structure was obtained on the basis of the dislocation model proposed. This makes it possible to trace the variation of FD of the dislocation cell structure with strain by simply measuring the macroscopic stress-strain curve.

A comparison of the FD behavior predicted for the bulk dislocation arrangement in a Ni single crystal with the FD evolution pertaining to the surface morphology provided support for the widespread belief that information about dislocation patterning in the bulk can be obtained by monitoring the development of the surface profile.

It was shown that FD of the bulk dislocation structure in a deforming metal peaks at a certain strain. The observation of a drop of FD towards the point of failure can be interpreted as an indication that the dislocation cell structure becomes progressively more ordered with approach to fracture. A similar behavior of FD was repeatedly reported in the Earth science literature, cf. [30].

We appreciate that seemingly good quantitative agreement of the experimentally measured FD values with the model predictions, Fig. 2, should not be overrated. The absolute values of the fractal dimension obtained by different methods can vary considerably [28,29,31]. Still, we would like to emphasize the remarkably good agreement obtained in this work with regard to the common trends in the behavior of experimentally measured and predicted FD. Hence, the significance of FD as a robust and informative index to follow the evolution of dislocation structures should not be underestimated.

Financial support from the Russian Ministry of Education and Science through the grant-in-aid No. 11.G34.31.0031 is greatly appreciated.

*Corresponding author.
On leave from Osaka City University, Osaka 558-8585, Japan.
vinogradov@tltsu.ru, alexei@imat.eng.osaka-cu.ac.jp

[1] B. B. Mandelbrot, *The Fractal Geometry of Nature* (W. H. Freeman, New York, 1983).
[2] M. Zaiser, F. M. Grasset, V. Koutsos, and E. C. Aifantis, Phys. Rev. Lett. **93**, 195507 (2004).
[3] M. Zaiser, K. Bay, and P. Hähner, Acta Mater. **47**, 2463 (1999).
[4] M. Zaiser, Adv. Phys. **55**, 185 (2006).
[5] O. Meissner, J. Schreiber, and A. Schwab, Appl. Phys. A **66**, S1113 (1998).
[6] P. V. Kuznetsov, V. E. Panin, and J. Schreiber, Theor. Appl. Fract. Mech. **35**, 171 (2001).
[7] I. Prigogine, *Introduction to Thermodynamics of Irreversible Processes* (Interscience, NY, 1961).
[8] M. Huang, P. E. J. Rivera-Díaz-del-Castillo, O. Bouaziz, and S. van der Zwaag, Mater. Sci. Technol. **24**, 495 (2008).
[9] J. P. Hirth and J. Lothe, *Theory of Dislocations* (Wiley, New York, 1982), 2nd ed.
[10] U. F. Kocks and H. Mecking, Prog. Mater. Sci. **48**, 171 (2003).
[11] L. P. Kubin *et al.*, in *Dislocations in Solids* (Elsevier, New York, 2002), p. 101.
[12] H. Mughrabi, J. Mater. Res. **97**, 594 (2006).
[13] H. Mughrabi, Acta Metall. **31**, 1367 (1983).
[14] D. L. Holt, J. Appl. Phys. **41**, 3197 (1970).
[15] Y. Estrin and H. Mecking, Acta Metall. **32**, 57 (1984).
[16] H. Mecking and U. F. Kocks, Acta Metall. **29**, 1865 (1981).
[17] U. F. Kocks, A. S. Argon, and M. F. Ashby, Prog. Mater. Sci. **19**, 1 (1975).
[18] N. Hansen and D. Kuhlmann-Wilsdorf, Mater. Sci. Eng. **81**, 141 (1986).
[19] Y. Estrin, L. S. Tóth, A. Molinari, and Y. Bréchet, Acta Mater. **46**, 5509 (1998).
[20] P. Hähner, K. Bay, and M. Zaiser, Phys. Rev. Lett. **81**, 2470 (1998).
[21] I. Groma and B. Bakó, Phys. Rev. Lett. **84**, 1487 (2000).
[22] M. Koslowski, R. LeSar, and R. Thomson, Phys. Rev. Lett. **93**, 265503 (2004).
[23] C. Y. J. Barlow, B. Bay, and N. Hansen, Philos. Mag. A **51**, 253 (1985).
[24] J. Christiansen, K. Morgenstern, J. Schiøtz, K. W. Jacobsen, K.-F. Braun, K.-H. Rieder, E. Lægsgaard, and F. Besenbacher, Phys. Rev. Lett. **88**, 206106 (2002).
[25] G. A. Malygin, Phys. Solid State **49**, 1460 (2007).
[26] K. Stout and L. Blunt, *Three-Dimensional Surface Topography* (Penton, London, 2000).
[27] K. J. Falconer, *Techniques in Fractal Geometry* (Wiley, Chichester, New York, 1997).
[28] B. Dubuc, J. F. Quiniou, C. Roques-Carmes, C. Tricot, and S. W. Zucker, Phys. Rev. A **39**, 1500 (1989).
[29] J. C. Russ, *Fractal Surfaces* (Plenum Press, New York, 1994).
[30] T. Hirata, T. Satoh, and K. Ito, Geophys. J. R. Astron. Soc. **90**, 369 (1987).
[31] U. Wendt, K. Stiebe-Lange, and M. Smid, J. Microsc. **207**, 169 (2002).